# QUENCHING OF SPECTROSCOPIC FACTORS IN $^{10,12}$Be PICK-UP TRANSFER REACTIONS*

M. Lozano-González, B. Fernández-Domínguez
J. Lois-Fuentes

IGFAE and Dpt. de Física de Partículas, Univ. of Santiago de Compostela
15758 Santiago de Compostela, Spain

A. Matta, F. Delaunay

Université de Caen-Normandie, ENSICAEN, CNRS/IN2P3
LPC Caen UMR6534, 14000 Caen, France

on behalf of the E748 Collaboration†

*Received 29 November 2024, accepted 11 December 2024, published online 10 April 2025*

The reduction of the experimental spectroscopic factors when compared to shell model calculations and its dependence on the binding energy asymmetry has puzzled researchers for more than a decade. As it is understood, short-range correlations among nucleons play an important role in this quenching. To shed more light on this topic, an experiment was performed at GANIL to determine the reduction factor $R_{\mathrm{S}}$ in $^{10}\mathrm{Be}(d,t)^{9}\mathrm{Be}$, $^{10}\mathrm{Be}(d,{}^{3}\mathrm{He})^{9}\mathrm{Li}$, and $^{12}\mathrm{Be}(d,{}^{3}\mathrm{He})^{11}\mathrm{Li}$ pick-up reactions. This work reports on the preliminary spectroscopic factors that will be used to extract $R_{\mathrm{S}}$, as well as a comparison and reanalysis of previous datasets for pick-up on $^{10}$Be. An agreement between our results and previously published data has been found, along with strong indications of a reduction factor in line with available systematics.

DOI:10.5506/APhysPolBSupp.18.2-A15

## 1. Introduction

In the mean-field picture, nucleons inside nuclei move in single-particle orbitals with well-defined energies and quantum numbers. This approach, yet describing many of the nuclear properties, fails to account for short-range correlations (SRCs) among nucleons. As a consequence, the experimental

* Presented at the 57$^{\mathrm{th}}$ Zakopane Conference on Nuclear Physics, *Extremes of the Nuclear Landscape*, Zakopane, Poland, 25 August–1 September, 2024.

† The list of E748 Collaboration members can be found at the end of the article.

spectroscopic factors (SFs) are found to be reduced by a 0.4 factor compared to the independent-particle shell model (SM) values. This results in the so-called quenching of the spectroscopic factors, known for three decades now [1].

Transfer reactions, in which a single nucleon is added to or removed from the target nucleus, provide a unique tool to probe the impact of those correlations on the single-particle strengths. The present experiment provides an update on the reduction factor for nuclei with large binding energy asymmetries $\Delta S = \pm(S_p - S_n)$ through the neutron $(-)$ or proton $(+)$ pick-up reactions $^{10}$Be$(d,t)^{9}$Be, $^{10}$Be$(d,^{3}$He$)^{9}$Li ($\Delta S = \mp 12.8$ MeV), and $^{12}$Be$(d,^{3}$He$)^{11}$Li ($\Delta S = +19.8$ MeV). This report shows preliminary angular distributions for all the states of interest, while the quenching factor will be the topic of a future extended article.

## 2. Experimental setup

The E748 experiment was carried out at the GANIL facility in 2017. Secondary $^{10,12}$Be beams were produced with intensities of $10^4$ pps to $10^5$ pps after the fragmentation of an $^{18}$O primary beam on a Be target. The isotope and energy selection of 30 $A$ MeV were achieved using the LISE spectrometer capabilities, which delivered them to a 2 mg/cm$^2$-thick deuterated polypropylene ($CD_2$) target.

Two low-pressure multiwire proportional chambers (CATS) [2] detectors were placed upstream of the target's position to precisely reconstruct the beam spot and enhance the overall resolution, whereas the light recoils were detected in 6 MUST2 [3] telescopes placed at 18 cm from the target: 4 of them span 10° to 50° in $\theta_{\text{lab}}$ and the remaining two measure the elastic scattering at 90°. Each telescope consists of a first stage made of a 300 $\mu$m-thick double-sided Si strip detector (DSSD), followed by a second stage of CsI crystals. Together, they provide the necessary kinematical parameters ($E$, $\theta_{\text{lab}}$) to reconstruct the excitation energy $E_x$ by the missing-mass technique. The setup is completed with a zero-degree detector (ZD): an ionization chamber and a plastic scintillator that provide an atomic number identification of the heavy residues.

## 3. Data analysis

Owing to the high purity of the delivered beams, no particular gates are needed for the beam particles and only a gate in the target position is applied to reject reactions with the target frame. Then, the ZD detectors are used to gate on the $Z$ of the residual nucleus, as shown in Fig. 1 (a). This figure shows the energy loss in the ionization chamber $\Delta E$ against the residual energy $E$ in the plastic scintillator, allowing for a clear separation of Be and Li isotopes.

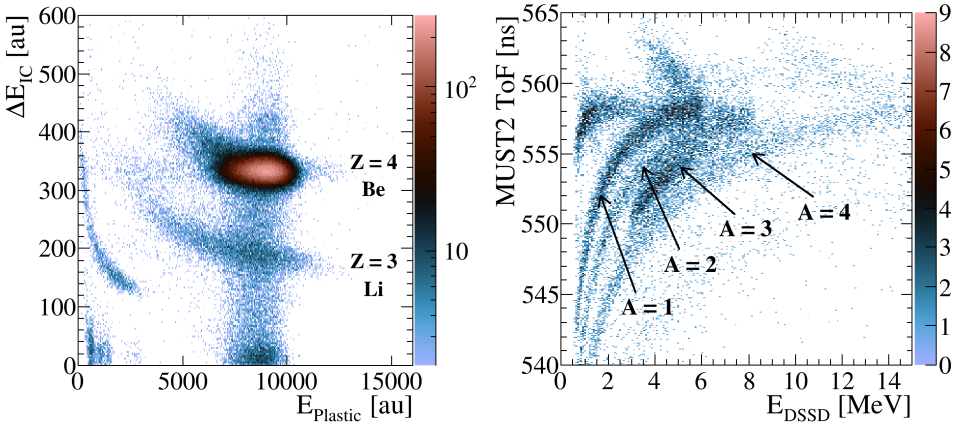


(a) Heavy residue selection (b) Light particle identification

Fig. 1. Particle identification in the ZD detectors (a) and in MUST2 (b).

Subsequently, the time capabilities of MUST2 are exploited to perform the light-particle identification. This is done through the time-of-flight (ToF) method, in which the ToF between the DSSD and the first CATS detector is plotted against the $E$ in the Si detector, as in Fig. 1 (b). The essential discrimination between the $(d,t)$ and $(d,^3\mathrm{He})$ channels is achieved with the previous selection of the heavy fragment in the ZD detector.

Regarding the angular distributions, these are obtained for the populated states in the $E_x$ spectrum by counting events in $\theta_{\mathrm{CM}}$ bins and correcting for efficiency losses, following the equation:

$$\left.\frac{\mathrm{d}\sigma}{\mathrm{d}\Omega}\right|_{\mathrm{exp}} \equiv \frac{N(\theta_{\mathrm{CM}})}{N_{\mathrm{beam}} N_{\mathrm{targets}} \epsilon(\theta_{\mathrm{CM}}) \Delta\Omega(\theta_{\mathrm{CM}})},$$

with $N_{\mathrm{beam}}$ the number of beam particles collected with the trigger, $N_{\mathrm{targets}}$ the number of deuterons in the target, and $\epsilon\Delta\Omega$ the solid angle efficiency, which includes both the geometric and the reconstruction algorithm losses.

In this experiment, the target thickness and the intrinsic efficiency of the ZD are not precisely known and therefore the elastic scattering is used to obtain an absolute normalization by defining the factor $\alpha = N_{\mathrm{targets}}\,\epsilon_{\mathrm{ZD}}$. This constant is determined from fits of theoretical elastic scattering cross-section calculations to our data and is applied in all subsequent analyses. This is shown in Fig. 2, which also compares results from different Optical Model Potential (OMP) parameterizations [4–6] to identify the best option based on the $\chi^2_{\mathrm{red}}$. For the $^{10}\mathrm{Be} + d$ case, Daehnick provides the best fit ($\chi^2_{\mathrm{red}} = 1.33$), while that of $^{12}\mathrm{Be} + d$ is better described by Haixia ($\chi^2_{\mathrm{red}} = 1.55$). The sensitivity of the normalization to the choice of OMP has been

estimated using the other OMP lines, yielding a deviation of 30% from the best model. This value will be considered a systematic uncertainty for the SF extracted in the following steps.

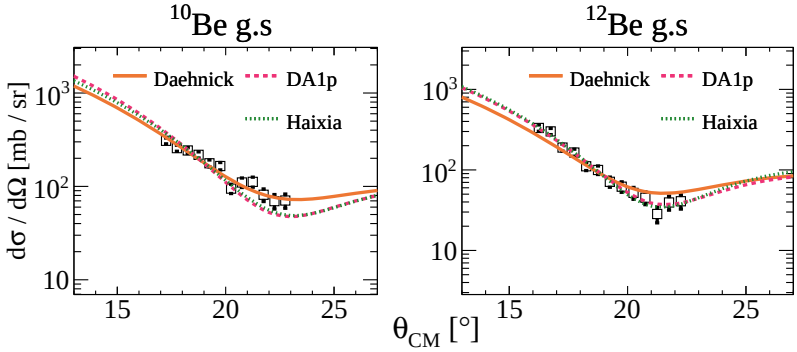


Fig. 2. $^{10}$Be and $^{12}$Be elastic scattering angular distributions and optical model calculations employing different OMPs, normalized to the data.

For the transfer channels, the SF is obtained by normalizing the single-particle cross section from a Distorted-Wave Born Approximation (DWBA) to the experimental data. These DWBA calculations were carried out with the finite-range FRESCO code [7]. In the incoming channel, the corresponding OMP determined from the elastic scattering is used, whereas in the outgoing channel, the HT1p potential [8] was employed. This choice is justified since the HT1p global parametrization includes nuclei around our mass region (the so-called 1$p$ nuclei, hence the suffix).

Lastly, the light particle $\langle t, {}^3\mathrm{He} \mid d \otimes n, p\rangle$ overlap was computed in a binding potential adjusted on results of Green's function Monte Carlo (GFMC) *ab initio* calculations [9], whilst the heavy particle overlap $\langle {}^{10,12}\mathrm{Be}| {}^{9,11}\mathrm{Be, Li} \otimes n, p\rangle$ was generated in a Woods–Saxon (WS) potential with a standard geometry: $r_0 = 1.25\,\mathrm{fm}$ and $a = 0.65\,\mathrm{fm}$.

## 4. Preliminary results

The preliminary experimental angular distributions for the accessible states of $^{10}\mathrm{Be}(d,t)^9\mathrm{Be}$, $^{10}\mathrm{Be}(d,{}^3\mathrm{He})^9\mathrm{Li}$, and $^{12}\mathrm{Be}(d,{}^3\mathrm{He})^{11}\mathrm{Li}$ are extracted and displayed in Fig. 3. They are compared with the DWBA calculations assuming different $\Delta L$ angular momentum transfers, providing $\Delta L = 1$ the best fits in all cases, in agreement with known $J^\pi$ assignments [10].

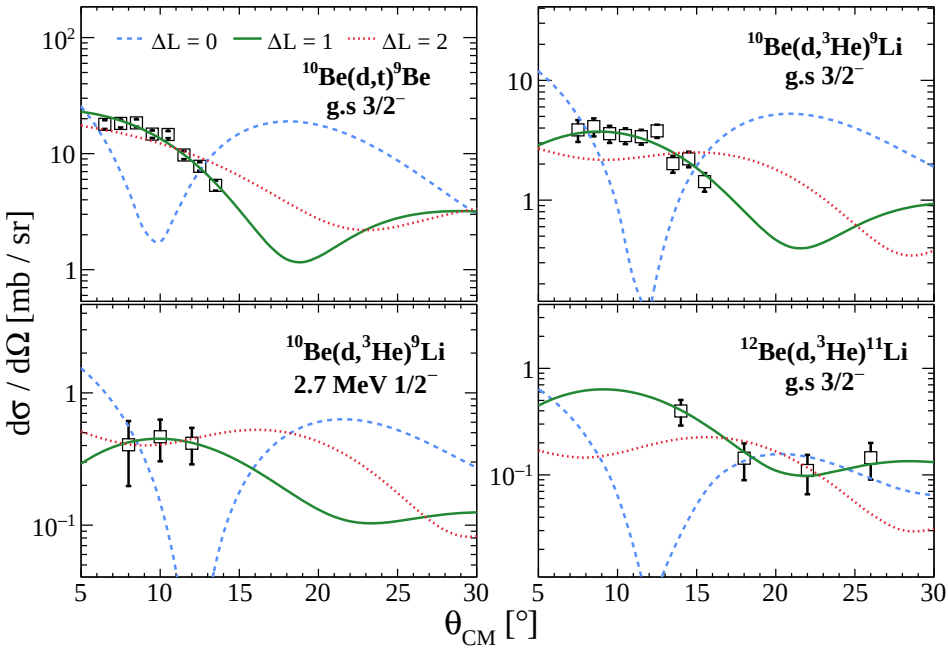


Fig. 3. Experimental angular distributions for the corresponding states compared to DWBA computations with different angular momentum transfers $\Delta L = 0, 1,$ and 2.

Table 1 presents the results of the SFs together with shell model calculations employing the SFO-tls interaction, which has already succeeded in describing other *p-sd* neutron-rich nuclei such as $^{17}$C [11, 12] or $^{15}$C [13]. These preliminary results already point out a strong reduction (in terms of the $SF_{exp}/SF_{SM}$ ratio) in line with expected values.

This table also shows SFs obtained in previous experiments at different beam energies. Their results are in strong disagreement with our values ($\sim 50\%$ differences), which could be due to having employed different OMP parameters. A reanalysis of their experimental data using instead our OMP is carried out and the results are depicted in Fig. 4. The new SFs agree quite well for the case of $^{9}$Be, while for $^{9}$Li some discrepancy is observed in the shape of the angular distributions. However, the reanalysed spectroscopic factor agrees well with our result within the systematic error bar.

Table 1. Excitation energies ($E_x$), spin-parities ($J^\pi$), angular momentum transfers ($\Delta L$), and both experimental ($SF_{exp}$) and shell model ($SF_{SM}$) spectroscopic factors for the states found in this study. Comparisons with reanalysis of previous data in [14, 15] are also shown. Uncertainty is expressed as (statistical)(systematic) components, considering for the systematic 30% value estimated in the elastic scattering comparison, while the statistical comes directly from the minimization procedure.

| | $E_x$ | $J^\pi$ | $\Delta L$ | $SF_{exp}$ This work | $SF_{exp}$ Previous | $SF_{SM}$ |
|---|---|---|---|---|---|---|
| $^{10}$Be$(d,t)^{9}$Be | g.s. | $3/2^-$ | 1 | 1.308(36)(390) | 1.682(49)(504)[a]<br>2.19(48) [14] | 2.511 |
| $^{10}$Be$(d,^3$He$)^{9}$Li | g.s. | $3/2^-$ | 1 | 0.927(49)(278) | 1.576(29)(473)[b]<br>1.74 [15] | 1.69 |
| | 2.7 MeV | $1/2^-$ | 1 | 0.154(45) | | 0.279 |
| $^{12}$Be$(d,^3$He$)^{11}$Li | g.s. | $3/2^-$ | 1 | 0.260(45)(78) | | 1.642 |

[a] Reanalysis of experimental data in [14].
[b] Reanalysis of [15].

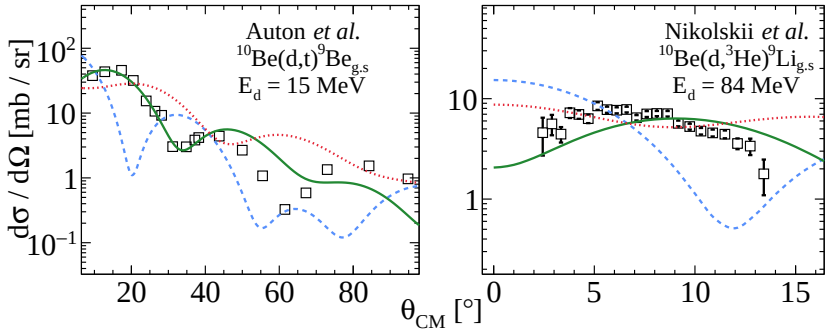


Fig. 4. Reanalysis of previous data in [14, 15]. Notation for graphs remains equal to the previous figure. Note that for [14], error bars could not be extracted from the original publication.

## 5. Summary and outlook

Spectroscopic factors have been deduced for $^{10}$Be$(d,t)^{9}$Be, $^{10}$Be$(d,^{3}$He$)^{9}$Li, and $^{12}$Be$(d,^{3}$He$)^{11}$Li reactions. Their preliminary values suggest a strong reduction, namely for the very asymmetric system $^{11}$Li.

In the future, the determination of the reduction factor will be contrasted with theoretical calculations in two approaches:

— Using shell model calculations with the state-of-the-art interactions such as the SFO-tls. In this case, we expect a reduction factor $\sim 0.4$ of the shell model strength, as the preliminary SF already indicate.

— An alternative approach to compute the heavy particle overlap $\langle \mathrm{A}|\mathrm{A}-1\rangle$: the Source Term Approach (STA) [16]. This method differs from the standard shell model in that it solves an inhomogeneous equation generating the overlap (that leads to the SF definition) by using an effective interaction (*source term*) and, this way, the results implicitly capture some of the $NN$ correlations. Instead, the shell model would return the SF by direct evaluation of wave-function products in truncated model spaces, losing radial information that is essential to account for correlations. Theoretical SFs computed with this method are available in [17] and will be compared with the present experimental data but using DWBA calculations with a heavy particle overlap reproducing the STA results.

The case of $\langle^{12}\mathrm{Be}|^{11}\mathrm{Li}\rangle$ requires further attention as there is a large difference in the binding energies of the valence neutrons between both nuclei ($S_{2n}(^{12}\mathrm{Be}) = 3.67\,\mathrm{MeV}$ and $S_{2n}(^{11}\mathrm{Li}) = 0.37\,\mathrm{MeV}$). It was shown in a previous experiment for the $\langle^{11}\mathrm{Li}|^{10}\mathrm{He}\rangle$ case that this translates into a radial (or *geometrical*) mismatch factor (GMF) that reduces the SF and could mask the quenching phenomenon [18]. This effect is also predicted for our case [19] and, consequently, the $^{12}$Be$(d,^{3}$He$)^{11}$Li reaction will be employed to constrain this key parameter.

M.L.G. wishes to acknowledge financial support from the Xunta de Galicia (Spain) grant number ED481A-2022/419. The Spanish MINECO supported this work through the project PID2021-128487NB-I00. This work was also partially funded by the Xunta de Galicia under projects 2021-PG045 and 2024-PG040, and the Maria de Maeztu Unit of Excellence CEX2023-001318-M.

## REFERENCES


[1] T. Aumann *et al.*, *Prog. Part. Nucl. Phys.* **118**, 103847 (2021).

[2] S. Ottini-Hustache *et al.*, *Nucl. Instrum. Methods Phys. Res. A* **431**, 476 (1999).

[3] E. Pollacco *et al.*, «MUST2: A new generation array for direct reaction studies», in: «The 4th International Conference on Exotic Nuclei and Atomic Masses», *Springer Berlin Heidelberg*, Berlin, Heidelberg 2005, pp. 287–288.

[4] W.W. Daehnick, J.D. Childs, Z. Vrcelj, *Phys. Rev. C* **21**, 2253 (1980).

[5] Y. Zhang, D.Y. Pang, J.L. Lou, *Phys. Rev. C* **94**, 014619 (2016).

[6] A. Haixia, C. Chonghai, *Phys. Rev. C* **73**, 054605 (2006).

[7] I.J. Thompson, *Comput. Phys. Rep.* **7**, 167 (1988).

[8] D.Y. Pang, W.M. Dean, A.M. Mukhamedzhanov, *Phys. Rev. C* **91**, 024611 (2015).

[9] I. Brida, S.C. Pieper, R.B. Wiringa, *Phys. Rev. C* **84**, 024319 (2011).

[10] «Evaluated Nuclear Structure Data File», `https://www.nndc.bnl.gov/ensdf/`, 2024.

[11] T. Suzuki, T. Otsuka, *Phys. Rev. C* **78**, 061301 (2008).

[12] X. Pereira-López *et al.*, *Phys. Lett. B* **811**, 135939 (2020).

[13] J. Lois-Fuentes *et al.*, *Phys. Lett. B* **845**, 138149 (2023).

[14] D.L. Auton, *Nucl. Phys. A* **157**, 305 (1970).

[15] E.Yu. Nikolskii *et al.*, *Nucl. Instrum. Methods Phys. Res. B* **541**, 121 (2023).

[16] N.K. Timofeyuk, *Phys. Rev. Lett.* **103**, 242501 (2009).

[17] N.K. Timofeyuk, *Phys. Rev. C* **88**, 044315 (2013).

[18] A. Matta *et al.*, *Phys. Rev. C* **92**, 041302 (2015).

[19] N.K. Timofeyuk, *J. Phys. G: Nucl. Part. Phys.* **41**, 094008 (2014).


The list of E748 Collaboration members: N.L. Achouri, M. Assié, B. Bastin, D. Beaumel, Y. Blumenfeld, M. Caamaño, W.N. Catford, A. Corsi, F. de Oliveira, N. de Séréville, F. Flavigny, S. Franchoo, A. Georgiadou, J. Gibelin, A. Gillibert, V. Girard-Alcindor, J. Guillot, F. Hammache, B. Jacquot, O. Kamalou, S. Koyama, V. Lapoux, A. Lemasson, G. Lotay, M. Marqués, A. Meyer, N.A. Orr, J. Pancin, E.C. Pollacco, M. Rejmund, T. Roger, O. Sorlin, I. Stefan, C. Stodel, D. Suzuki, J.C. Thomas, N.K. Timofeyuk, R. Wilkinson.